ESTIMATION OF GEOMETRIC RADAR CONFIGURATION PARAMETERS FOR RANGE-DEPENDENT COMPENSATION IN STAP IN THE PRESENCE OF TARGETS, JAMMERS, AND DECORRELATION EFFECTS

Xavier Neyt, Fabian D. Lapierre (Research fellow)†, Jacques G. Verly†*

*Royal Military Academy, Department of Electrical Engineering,
Avenue de la Renaissance, 30, B-1000, Bruxelles, Belgium
†University of Liège, Department of Electrical Engineering and Computer Science,
Sart-Tilman, Building B28, B-4000 Liège, Belgium

ABSTRACT

We propose a new method for extracting the geometric radar configuration parameters required to perform range-dependence compensation of clutter statistics in space-time adaptive processing (STAP). The performance of the method is evaluated in the presence of targets, jammers, and decorrelation effects, such as due to internal clutter motion.

1. INTRODUCTION

We consider space-time adaptive processing (STAP) for both monostatic (MS) and bistatic (BS) radar configurations. For STAP to reduce the interference caused by ground clutter and jammers, the interference-plus-noise (I+N) covariance matrix (CM) must be estimated for each range.

The standard method for estimating the I+N CM is to average the single-sample CM at various ranges around each range of interest. This average is called the sample CM [1]. Below, we generically refer to the power spectral density PSD estimates of the STAP snapshot as the I+N (or simply clutter) power spectrum (PS). The averaging of the single-sample CMs provides an accurate estimate in MS sidelooking configurations, where the clutter PS does not depend upon range. For all other configurations, the clutter PS exhibits a significant range dependence, hence resulting in an incorrect CM estimate. The clutter PS can also be viewed as a continuous function of range. In other words, "stacking" 2D clutter PS as a function of range results in a 3D clutter PS. For conciseness, when no confusion is likely to arise, we will often drop "clutter" when talking about a PS.

Reference [2] describes a method for taking into account the range-dependence of the PS in performing the averaging. This method relies on the knowledge of the variation with range of the 2D PS. The method estimates the configuration parameters, i.e., the receiver location (R, θ, ϕ) relative to the transmitter, the transmitter velocity v_T, the receiver velocity v_R, the receiver velocity direction α_R relative to the emitter velocity direction, and the antenna azimuth δ. However, the method is intended for use with omnidirectional antenna configurations and in the absence of other interferers, or decorrelation effects.

In this paper, we propose a new method capable of estimating the locus of the 3D PS from single realizations of the I+N snapshots at all available ranges. The method is shown to be robust to the presence of other interferers, such as targets and jammers, and decorrelation effects.

In Section 2, the estimation method is described. In Section 3, the artifacts of interest are modeled and their effect on the performance of the new method is discussed. Conclusions are drawn in Section 4.

2. NEW PARAMETER ESTIMATION METHOD

The main motivation for this estimation method is that the energy of the single-realization 2D PS is concentrated along a curve, in the spatial-Doppler frequency plane, that only depends on the configuration parameters. Indeed, by definition, the scatterers contributing to clutter are located on the isorange corresponding to each BS range of interest. To each scatterer at a specific position along this isorange correspond specific spatial and Doppler frequencies and hence a specific location in the spatial-Doppler frequency plane. As one considers a succession of points along the isorange, one creates a succession of corresponding points and, thus, a curve in that frequency plane. The analytic expression for this curve, i.e., for the theoretical locus of the 2D PS, can be obtained by eliminating the coordinates of the scatterer between the parametric equations of the isorange and the equations giving the spatial and Doppler frequencies. Various quantities of interest are illustrated in Fig. 1. The presence of "peaks" in the 2D PS is a result of modeling scatterers as backscattering signals with a random, uniformly-distributed phase. When the loci of the 2D PS at different ranges are stacked on top of each other, the theoretical locus

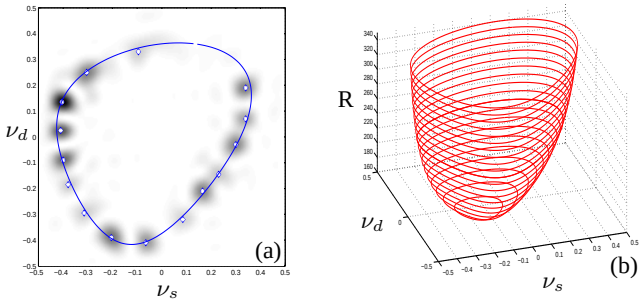

Fig. 1. (a) The grayscale image shows the 2D PS of one particular snapshot realization. The black line is the true theoretical locus of the PS. The white dots indicate the positions of the peaks of the PS. (b) 3D view of the theoretical locus of the PS as a function of range.

of the 3D PS is obtained, which is of course a 3D surface. Due to the range dependence, this surface deviates considerably from a vertical cylinder, as is illustrated in Fig. 1(b).

The parameter estimation method consists in fitting the mathematical model of the theoretical 3D PS locus to the experimental 3D PS. First, the 2D PS is obtained by computing the periodogram of the snapshot data. Since the zero-padding that is applied to the snapshot data (in order to increase the frequency resolution) has the effect of smoothing the 2D PS, the location of the peaks can be obtained by extracting local maxima. Only the largest local maxima are kept, thus discarding spurious peaks. The result of this process is indicated by the white dots in Fig. 1(a).

The next step consists in fitting the model of the theoretical 3D PS locus to the extracted peaks. Note that the model is valid for all ranges and that the fit is performed for all ranges at the same time.

The accuracy of the fit is measured by a cost function defined as the RMS of the distances of the peaks to the estimated theoretical 3D PS locus (i.e., corresponding to the estimated parameters). In order to discard spurious peaks (due for instance to targets), only the peaks "close" to the estimated theoretical 3D PS locus are retained. Furthermore, the contribution of each peak to the value of the cost function is weighted by the amplitude of this peak, with the justification that "small-amplitude" peaks are more likely to be due to some artifacts.

The configuration parameters are determined by minimizing the cost function using a variant of the simplex method. This method offers the advantage that the derivatives of the cost function do not have to be explicitly computed. The estimation method and the minimization of the cost function are more extensively described in [3].

3. PERFORMANCE IN NONIDEAL CASES

We now discuss the ability of the configuration parameters estimation method to converge correctly to the true theoretical 3D PS locus (i.e., corresponding to the true parameters) in the presence of various undesirable artifacts. The undesirable artifacts discussed below are targets, jammers, and decorrelation effects.

The BS scenario used to illustrate this section comprises a transmitter located at the origin, 50km above ground, a receiver located at $(80, 50, 20)$km. The transmitter velocity is of 90m/s in the x-direction, while the receiver velocity is also of 90m/s, but in a direction making an angle of 35^o with the x-axis. The crab angle of the receiver antenna is of 60^o.

The method used to estimate the CM is a variant of the registration-based compensation (RBC) method presented in [2]. The configuration parameters required by the RBC method are estimated using the new method proposed in this paper.

3.1. Targets

A target appears as a concentration of energy at a specific point in the spatial-Doppler frequency spectrum. Its exact location depends on the relative position and velocity of the target and the transmitter/receiver pair.

Targets usually appear in one range bin only. Extended targets might leak into neighboring range bins. As far as the estimation method is concerned, each target thus appears as one peak in one particular range bin and, possibly, in neighboring range bins.

Since the estimated theoretical 3D PS locus is constrained to a particular mathematical model, the only influence targets can have is through their contribution to the cost function. Indeed, peaks located "far" from the estimated theoretical 3D PS locus are rejected and do not contribute to the cost function. Furthermore, since most peaks correspond to clutter, the presence of a few extra peaks due to targets does not have a large impact on the value of the cost function.

We conclude that the estimation method is highly insensitive to the presence of targets in the training snapshots.

Figure 2 shows the PS of the estimated I+N CM obtained, in the presence of a target, using (a) the sample CM [1] and (b) the RBC method. The scenario of interest consists of a target located at boresight of the receiving antenna and positioned to yield an echo at a range smaller than the range of interest. The target thus contaminates the secondary snapshots, i.e, those used to compute the sample CM. The target is clearly visible near zero azimuth and zero Doppler in the PS of the sample CM while it is absent in the PS of the I+N CM estimate obtained using the RBC method. However, even though the influence of the target on

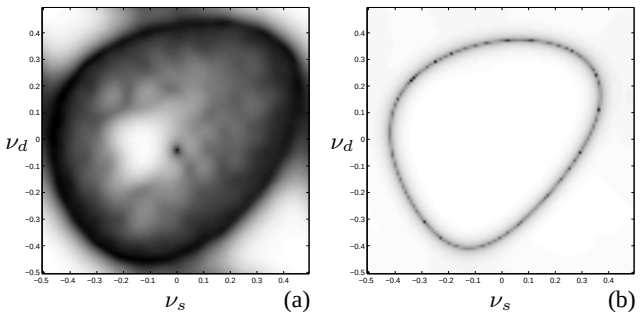

Fig. 2. PS of the I+N CM estimated using (a) the sample CM and (b) the RBC method.

the sample CM is undesirable, this should not be confused with self-nulling.

Figure 3 presents the SINR loss obtained with the RBC

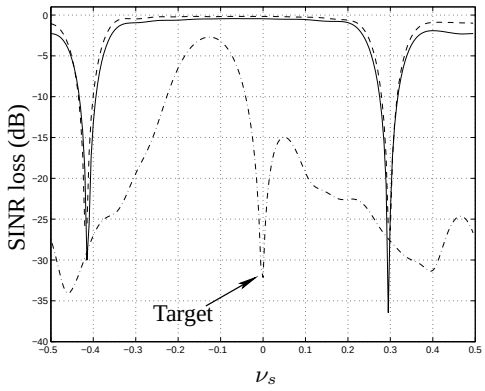

Fig. 3. SINR loss at $\nu_d = -0.04$ in the presence of one target in secondary training data.

method. The dashed-dotted line is the SINR loss obtained with the sample CM, i.e., using the sample matrix inversion (SMI) method [1]. The deep null near zero azimuth angle is due to the presence of the target in the training set. Moreover, as expected, the clutter interference is under-nulled due to the range-dependence effect. The solid line is the SINR loss obtained with the CM estimated using the RBC method. As a reference, the dashed curve shows the SINR loss obtained when the true CM is used, thus yielding the Optimum Processor (OP). The new method proposed thus yields results very close to the optimum.

3.2. Jammers

As in [4, 5], barrage jammers are now considered. One barrage jammer source is modeled as producing a received signal that is spatially correlated from antenna array element to antenna array element but temporally uncorrelated from pulse to pulse. Consequently, the 2D PS of a barrage jammer signal is perfectly localized in space and, thus, in spatial frequency, whereas the same signal spans the whole Doppler spectrum.

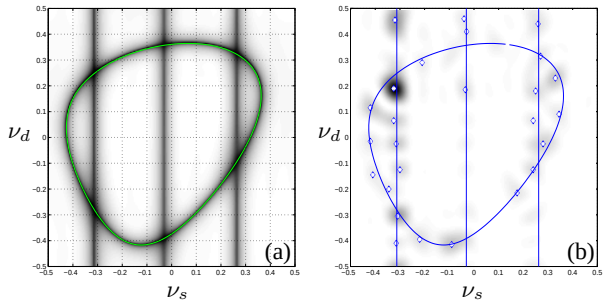

Fig. 4. 2D PS with clutter and 3 jammers. (a) "True" PS computed from the exact CM and (b) PS computed from a single snapshot.

Compared to targets, jammers create about as many peaks as clutter does in the 2D PS computed for a single random snapshot. Hence, the presence of the jammer peaks cannot be ignored as far as the fitting of the model for the theoretical 3D PS locus is concerned. Thus, before being able to fit the model of the theoretical (clutter) 3D PS locus, the energy contribution of the jammers must be suppressed.

If the (jammers + clutter) 2D PS corresponding to different ranges are stacked on top of each other, the energy of jammers appears as vertical planes at discrete spatial frequencies. This is illustrated in Fig. 5(a), which clearly shows that some peaks are clustered in 3 vertical planes corresponding to the 3 jammers.

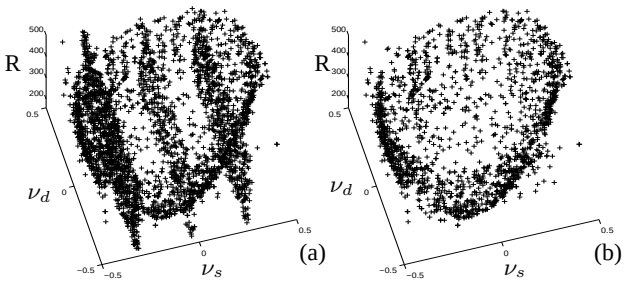

Fig. 5. Peaks extracted from a 3D PS for a 3-jammers scenario (a) with jammer peaks present and (b) with jammer peaks removed.

The method used to detect jammers is similar to that used to estimate the configuration parameters. First, the peaks are extracted from the 2D PS. This step is repeated for all ranges. Next, a set of planes parameterized by their spatial frequency is fitted to the extracted peaks. Since the number of jammers is unknown a-priori, the number of planes to consider is also unknown. In order to be sure to detect all jammers, a relatively large number of planes is considered.

Only a few of these will correspond to actual jammers. According to the jammer model described above, peaks due to jammers should be uniformly distributed in Doppler frequency. This property is used to select the planes that actually correspond to jammers. Peaks located close to the jammer planes are subsequently removed. In the example of Fig. 5, we used 5 planes for 5 hypothetical jammers. The remaining peaks can then be used as input to the configuration parameter estimation method described in Section 2.

Figure 6 shows the PS of the estimated I+N CM in the presence of barrage jammers. The 3 jammers are clearly

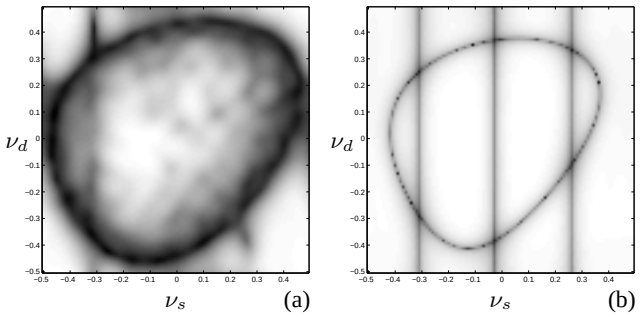

Fig. 6. PS of the I+N CM, estimated, in the presence of barrage jammers, using (a) the sample CM and (b) the RBC method.

visible in the PS of the estimate obtained using the RBC method while they are mostly absent from the PS of the sample CM. The most powerful jammer (on the left) is the most visible, having the same SNR as the clutter. The other jammers have a smaller SNR and are hardly visible in the PS of the sample CM.

Figure 7 presents the SINR loss obtained with the RBC

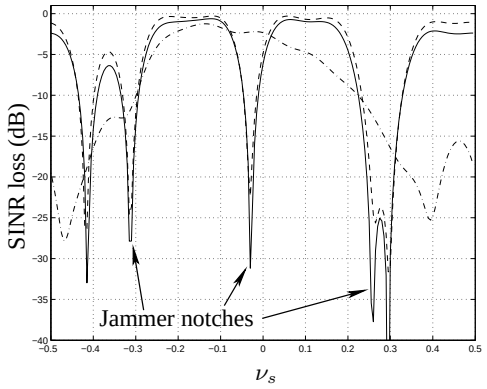

Fig. 7. SINR loss at $\nu_d = -0.04$ in the presence of 3 barrage jammers.

method for the 3-jammer scenario described above. The dashed-dotted line is the SINR loss obtained using the SMI method. The SMI method fails to correctly null the jammers and, again, as expected, the clutter interference is undernulled due to the range dependence of the clutter PS. The solid line represents the SINR loss obtained using the CM estimated using the RBC method. The dashed line shows the SINR loss obtained using the true (theoretical) I+N CM (OP). The RBC method yields results close to the optimum even in the presence of barrage jammers. Moreover, it is able to tackle simultaneously the range dependence of the clutter PS and the range-independent jammer PS.

3.3. Decorrelation effects

Several real-world phenomena result in a decorrelation of the received signal [5, 6, 7]. One distinguishes between *spatial decorrelation*, caused, e.g., by a finite system bandwidth or by antenna element position errors, and *temporal decorrelation*, caused by internal clutter motion (ICM), such as due to waves or tree leaves, or by range walk. The autocorrelation function of the decorrelated signals is either angle independent, in the case of ICM, or angle dependent, in the case of finite system bandwidth or range walk. In the latter cases, the decorrelation can still be assumed to be angle independent in the case of antennas with directional beampatterns.

The effect of decorrelation is a widening of the clutter ridge, which is dictated by the correlation function. The widening occurs in the spatial (temporal) direction if spatial (temporal) decorrelation effects are considered. As a consequence, the 2D PS is not concentrated along the theoretical 2D PS locus, but it is spread in its neighborhood. The configuration parameter estimation method described in Section 2 works by fitting a model to the data. Minimizing the distances between the extracted peaks and the estimated theoretical 3D PS forces the model to converge to a "mean" position. Since the pulse-to-pulse or element-to-element autocorrelation function is necessarily symmetric around zero, the estimated model will approach the true model, provided enough peaks are available. The new proposed configuration parameter estimation method is thus highly insensitive to decorrelation effects. To illustrate this, simulations were performed. A uniformly-distributed ICM (temporal decorrelation) was simulated. The maximum ICM ranges from 0 to 0.12 (normalized frequency units in the range $[-0.5, 0.5]$). Since we are essentially concerned with the estimation of the clutter PS locus, the shape of the PSD of the random phase jitter is not critical. Even thought we have considered a uniform PSD function, which is consistent with what is done in [7], an exponential PSD would be more realistic [8]. Figure 8(a) shows the RMS error between the estimated model and the true model as the maximum ICM increases. Figures 8(b) and 8(c) each show the true clutter PS locus and the estimated clutter PS locus for a maximum ICM of 0.01 and of 0.07, respectively. One can see that the estimation is quite accurate, even in the presence

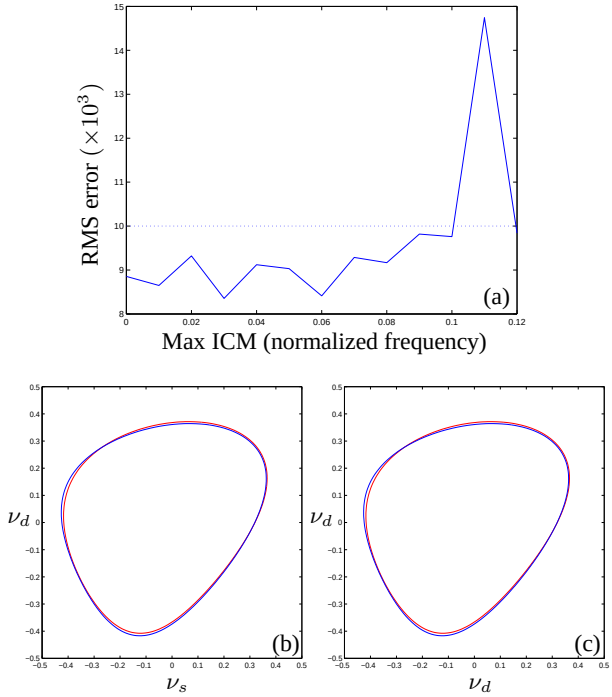

Fig. 8. (a) RMS error as a function of the max ICM. (b) True and estimated clutter PS locus for a max ICM of 0.01. (c) Same for a max ICM of 0.07.

of high ICM.

Figure 9 shows a comparison of the SINR loss obtained with different CM estimates. The dashed-dotted lines corresponds to the SINR loss obtained using the SMI method and the dashed line corresponds to the SINR loss obtained using the OP. The solid line is the SINR loss obtained using the RBC method. In the latter case, the distribution of the random phase jitter is assumed to be known.

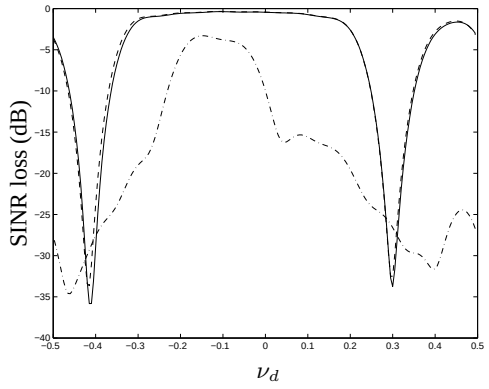

Fig. 9. SINR loss at $\nu_s = 0.0$ in the presence of ICM.

4. CONCLUSIONS

The new method proposed for configuration parameter estimation for range-dependence compensation in STAP was shown to be inherently insensitive to targets, jammers, and decorrelation effects. In conjunction with the range compensation method described in [2], the I+N covariance matrix for any MS or BS radar configuration can be estimated. With this matrix at hand, near-optimum target detection can be performed, which is, of course, the ultimate goal of STAP. The results in terms of SINR losses were shown to be nearly undistinguishable from those obtained with the optimum processor, which uses the true I+N covariance matrix.

5. REFERENCES

[1] I. S. Reed, J. D. Mallett, and L. E. Brennan, "Rapid convergence rate in adaptive arrays," *IEEE Transactions on Aerospace and Electronic Systems*, vol. 10, no. 6, pp. 853–863, Nov. 1974.

[2] F. D. Lapierre and J. G. Verly, "Registration-based solutions to the range-dependence problem in STAP radars," in *Adaptive Sensor Array Processing (ASAP) Workshop*, MIT Lincoln Laboratory, Lexington, MA, Mar. 2003.

[3] X. Neyt, F. D. Lapierre, and J. G. Verly, "Principle and evaluation of a registration-based range-dependence compensation method for STAP in case of arbitrary antenna patterns and simulated snapshots," in *Proc. Adaptive Sensor Array Processing Workshop*, MIT Lincoln Laboratory, Lexington, MA, Mar. 2004.

[4] J. Ward, "Space-time adaptive processing for airborne radar," Tech. Rep. 1015, MIT Lincoln Laboratory, Lexington, MA, Dec. 1994.

[5] Richard Klemm, *Principles of space-time adaptive processing*, The Institution of Electrical Engineers (IEE), UK, 2002.

[6] J. R. Guerci, *Space-Time Adaptive Processing for Radar*, Artech House, Norwood, MA, 2003.

[7] J. R. Guerci, "Theory and application of covariance matrix tapers for robust adaptive beamforming," *IEEE Transactions on Signal Processing*, vol. 47, no. 4, pp. 977–985, Apr. 1999.

[8] P. Lombardo and J.B. Billingsley, "A new model for the Doppler spectrum of windblown radar ground clutter," in *Record of the 1999 IEEE Radar Conference*, Boston, MA, pp. 142–147, Apr. 1999.